



# Development of angle-resolved low coherence interferometry for clinical detection of dysplasia

Yizheng Zhu, Neil G. Terry, Adam Wax\*

Department of Biomedical Engineering, Duke University, Durham, NC, USA

E-mail: a.wax@duke.edu

\*Corresponding author

Published: 23 August, 2011

Journal of Carcinogenesis 2011, 10:19

This article is available from: <http://www.carcinogenesis.com/content/10/1/19>

© 2011 Zhu,

Received: 28 March, 2011

Accepted: 24 June, 2011

### Abstract

This review covers the development of angle-resolved low coherence interferometry (a/LCI) from initial development through clinical application. In the first applications, the approach used a time-domain interferometry scheme and was validated using animal models of carcinogenesis to assess the feasibility of detecting dysplasia *in situ*. Further development of the approach led to Fourier-domain interferometry schemes with higher throughput and endoscope-compatible probes to enable clinical application. These later implementations have been applied to clinical studies of dysplasia in Barrett's esophagus tissues, a metaplastic tissue type that is associated with an increased risk of esophageal adenocarcinoma. As an alternative to systematic biopsy, the a/LCI approach offers high sensitivity and specificity for detecting dysplasia in these tissues while avoiding the need for tissue removal or exogenous contrast agents. Here, the various implementations of a/LCI are discussed and the results of the preliminary animal experiments and *ex vivo* human tissue studies are reviewed. A review of a recent *in vivo* clinical study is also presented.

**Keywords:** Barrett's esophagus, cell morphology, endoscopy, optical techniques

### INTRODUCTION

Light scattering spectroscopy has been shown to be a powerful, noninvasive way to determine the subcellular structure of tissue samples. Using advanced analysis and signal processing, light scattering measurements can provide quantitative data on nuclear morphology. These approaches

have been developed primarily for clinical use in the identification of biomarkers for dysplasia. Here, we review the development of angle-resolved low coherence interferometry (a/LCI), a novel depth-resolved light scattering method, and the role of animal models of carcinogenesis, in particular, the rat esophagus carcinogenesis model. The successful development of a/LCI demonstrates the important role of these models in developing diagnostic methods before application in humans.

Animal models have long been used in cancer research for their unique capacity to experiment with the carcinogenesis process in a way that is not possible in humans. The wide variety of animal models that serve as surrogates for human cancers has led to the development of chemopreventive and chemotherapeutic agents that retard or regress malignant

#### Access this article online

Quick Response Code:



Website:

[www.carcinogenesis.com](http://www.carcinogenesis.com)

DOI: 10.4103/1477-3163.83935

change. Small animal models have also provided suitable targets in the development of optical imaging techniques.<sup>[1-3]</sup> Work by our group and others has shown that light scattering measurements can be used for detecting neoplastic change in animal models.<sup>[4-6]</sup> Significantly, these techniques provide information on the health of epithelial tissues without the need for biopsy and histopathologic evaluation. These noninvasive, label-free techniques have also shown that changes can be detected earlier than with histopathology, notably, before any visible lesions appear.<sup>[7,8]</sup>

This review describes the development of a/LCI and its application to monitoring neoplastic progression through measurements of nuclear morphology. The a/LCI approach provides nuclear morphology information by analyzing the angular distribution of backscattered light. In a/LCI, depth resolution is obtained using coherence gating as in optical coherence tomography (OCT), a cross-sectional imaging technique.<sup>[9,10]</sup> However, a/LCI is distinct from OCT in that it can provide structural measurements that exceed the resolution of OCT by examining scattered light. The optical sectioning capability of a/LCI enables measurement of the morphology of basal cell nuclei, where neoplastic change originates.

The remainder of this review is organized as follows. First, an overview of a/LCI instruments is presented, including overviews of the optical systems. This is followed by a review of the evaluation of neoplastic transformation in animal models of carcinogenesis using nuclear morphology measurements. Finally, a review of the application of a/LCI to examining *ex vivo* and *in vivo* human tissues to demonstrate the relevance of the animal models is presented.

## INSTRUMENTATION

### Angle-resolved low coherence interferometry

As mentioned above, a/LCI is a light scattering technique that combines light scattering spectroscopy with the depth-sectioning capability of OCT.<sup>[10]</sup> The quantitative nuclear morphology obtained with a/LCI has been demonstrated to be effective for the assessment of tissue health.<sup>[4,11,12]</sup> As a noninvasive and label-free “optical biopsy” method, the a/LCI technique has shown great potential in assisting physicians in conventional biopsy procedures to improve detection accuracy and efficiency.<sup>[12]</sup>

Rather than directly imaging tissue structure, a/LCI measures the angular intensity distribution of light scattered by a tissue sample as a function of depth.<sup>[13]</sup> For each depth layer, the angular scattering signal is processed to extract

signatures from cell nuclei and then compared to a database of theoretical predictions. The best matching prediction produces highly accurate measurements of the mean size and relative refractive index of cell nuclei within the interrogated tissue volume.<sup>[14-16]</sup>

For most a/LCI analysis, the theoretical predictions were based on Mie theory, an analytical solution for the scattering of light from spherical particles.<sup>[17]</sup> Mie theory is particularly useful for the accurate analysis of scattering from wavelength-scale objects, and hence serves well as the numerical model for studying cellular and subcellular structures including nuclei.<sup>[14,18-23]</sup> It should be noted that Mie theory calculates scattering for homogenous spheres, while for most cells in culture or tissue, the nucleus is rather a prolate spheroid with irregular surfaces. These irregularities, however, are not correlated from nucleus to nucleus, but may instead be viewed as perturbations relative to an “average” cell nucleus. This is a relevant picture for a/LCI which averages the scattering of several hundred cells in a single measurement. The ensemble average of scattering from such a large number of cells serves to average out cell-to-cell variations, yielding a light scattering distribution closely characteristic of an average spherical nucleus. This is a desirable and necessary feature of this approach for determining nuclear morphology by comparison to Mie theory.

Before comparing and determining a size, the raw a/LCI signals are prepared through a series of pre-processing steps, notable among which are low-pass filtering and background trend subtraction.<sup>[14, 16]</sup> The former step suppresses high-frequency components stemming from long-range, intercellular correlations; the latter removes low-frequency contributions including those from inhomogeneities within the nucleus and smaller organelles within the cell. The preprocessing extracts the oscillatory component of light scattering which is characteristic of the nucleus size, which is then compared to Mie theory database to determine the average size and density of the nuclei.

With this nuclear morphology information, there is a wide spectrum of possible biological and medical applications for a/LCI. Previous studies have spanned from characterization of cultured cancer cells to detection of dysplasia in Barrett’s esophagus (BE) patients. In studies of neoplasia using multiple animal models, a/LCI has provided high sensitivity and specificity in differentiating non-dysplastic and dysplastic tissues.<sup>[6,24-26]</sup> Notably, it has been found that as tissue transforms from normal to dysplastic, the average cell nuclei size increases.<sup>[4,6,11]</sup> More significantly, a recent clinical study with *in vivo* data taken from human esophagi had similar findings.<sup>[12]</sup>

Responsible for each new, demanding application are the subsequent advances in a/LCI instrumentation. Higher speed and signal quality, better portability, and clinical compatibility are the key objectives that have been actively sought in a/LCI development, leading to tremendous scientific and engineering advancement across several generations of a/LCI hardware over the past decade. Among them, the quantum leap represented by the transition from a time-domain to Fourier-domain architecture, as well as the incorporation of an endoscopic fiber probe, has paved way for the current clinical application of the a/LCI technique. Here, we briefly review these developments.

### Early time-domain implementation

All a/LCI techniques rely on optical interferometry to detect a weak scattering signal from selected depths in tissue. Hence, the optical engine in each a/LCI system comprises an optical interferometer. Based on the type of interferometric technique used to obtain depth sectioning, a/LCI systems can be divided into two categories. The first of these techniques is a time-domain approach, which is similar to that used in time-domain OCT and was adopted in early a/LCI implementations.<sup>[13,15]</sup> The other is a Fourier-domain scheme, which forms the basis of recent a/LCI systems and will be introduced in the next subsection.

The first-generation time-domain a/LCI employed an optical engine based on a Michelson interferometer, with a high-level schematic shown in Figure 1a.<sup>[13]</sup> In this scheme, light from a broadband source is split into a reference beam, which remains in the optical engine, and a sample beam, which is sent externally to illuminate the tissue. Scattering from the tissue is collected and returned to interact with the reference, whose function is twofold: 1) it optically amplifies weak tissue scattering to enhance single-to-noise ratio (SNR) and 2) more importantly, it selectively detects scattering from a specific depth in the tissue. Scanning over a range of depths was achieved by a movable mirror (M) in the reference beam path. Angular scanning was accomplished in a similar fashion by the use of a translating lens (L).

This implementation was used to validate the concept of a/LCI and show that comparison of angular scattering intensity to Mie theory calculations resulted in an accurate measurement of average scatter size.<sup>[13]</sup> However, the mechanical movement of the mirror and the lens limited its potential applications due to low data acquisition speed. It could take up to 40 minutes to acquire one set of data (full angular signature at each depth layer) for a 1-mm<sup>2</sup> probed spot on a sample.

Aimed to significantly improve system speed and signal

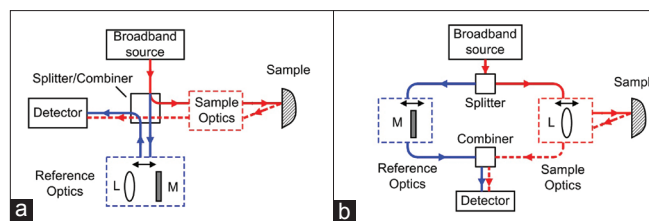


**Figure 1: Schematics of time-domain a/LCI systems. (a) First-generation implementation based on a Michelson interferometer where a single splitter/combiner splits and recombines signals. Mechanical movement of a mirror (M) and a lens (L) in the reference arm is necessary to scan over the full angular and depth range. (b) Second-generation system based on a Mach-Zehnder interferometer, where the splitter and combiner are separate elements. The movable mirror (M) and lens (L) are located differently, but perform the same depth/angular scanning functions as in (a)**

quality, the second-generation time-domain a/LCI employed a Mach-Zehnder interferometer (MZI) geometry [Figure 1b], which made possible the integration of a high-frequency heterodyne detection scheme.<sup>[15]</sup> Together with a high-power Ti:Sapphire laser source, this new scheme delivered larger dynamic range and allowed for much faster depth and angular scanning with the same movable mirror and lens, reducing data acquisition to approximately 5 minutes.

### Fourier-domain a/LCI implementation

When Fourier-domain techniques in OCT were first demonstrated to have SNR and speed advantages over their time-domain counterparts,<sup>[27]</sup> the concept was also introduced into a/LCI,<sup>[16,28-30]</sup> where the spectrum, rather than intensity, of the mixed reference and sample signal was acquired to recover sample information at all depths simultaneously, thereby eliminating the need for a moving mirror. Furthermore, Fourier-domain a/LCI also benefits from the use of an imaging spectrometer, a device capable of acquiring multiple spectra in parallel from all scattering angles without the need for a translating lens.

Without mechanical scanning, the Fourier-domain a/LCI system operates more stably and needs only a single readout from the imaging spectrometer to obtain one full data set. Consequently, the acquisition time for such a system can be as short as 20 milliseconds, limited only by the speed of the imaging spectrometer. The same data that initially required 40 minutes to acquire with the first-generation time-domain system can now be acquired  $\sim 10^5$  times faster. The feasibility of Fourier-domain a/LCI was first established using a bench-top MZI-based implementation.<sup>[28]</sup>

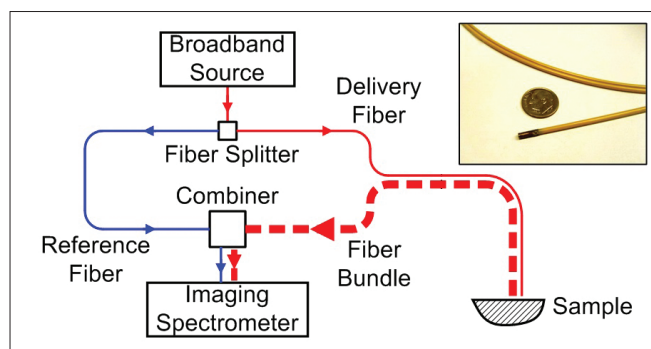
More recently, an endoscopic a/LCI system was developed to incorporate a thin, flexible fiber bundle in order to examine samples that are difficult to access otherwise.<sup>[29]</sup> Depicted in

Figure 2, this system used a single fiber to deliver illumination from the instrument box to the sample and a collocated fiber bundle to collect the scattering signal. Inside the bundle, independent fibers (~18,000 in total with ~150 active) receive light scattered at all angles and transmit them to the imaging spectrometer for parallel detection. Most other key components, such as the beam splitter, were also converted into fiber optics.

To take advantage of the compactness of fiber optics, a portable a/LCI system was soon built in a  $2 \times 2$  ft<sup>2</sup> instrument enclosure.<sup>[16]</sup> Resting on a lab cart, the enclosure housed most optical and electronic components. On the outside, a handheld fiber probe connected to the instrument enabled easy access to tissue samples for testing. These features allowed the system to be transported to a pathology lab for fast and selective scanning of resected tissue from human esophagi.

Most recently, significant engineering improvements have led to a clinical a/LCI system for *in vivo* examination of human subjects.<sup>[12,30]</sup> With an increasingly reduced footprint and weight, the system features a 2.5-mm-diameter, 230-cm-long fiber bundle probe, which is compatible with the accessory channel of a standard, 105-cm working distance endoscope. Under the visual guidance of the endoscope, the probe is placed in contact with the tissue during measurements to provide a consistent geometrical interface. A protective optical window permits the delivery of illumination to the tissue and the collection of scattered light by the distal end of the fiber bundle. The signal is then sent inside the optical engine for optical processing and readout.

This clinical system provides a point measurement that covers a tissue area of approximately 400  $\mu$ m in diameter, corresponding to the size of the illumination beam. Into the tissue, it can retrieve scattering information from beyond 500  $\mu$ m with a depth resolution of 26  $\mu$ m. To examine larger



**Figure 2: Schematic of the fiber-optic Fourier-domain a/LCI system with an endoscopic probe. Inset photo shows the probe in the clinical a/LCI system compared to a US dime**

tissue area, the a/LCI probe can be manually positioned to scan multiple sites, with a future possibility of mechanically scanning the beam with an integrated mirror to enhance operating speed.

Significant development of a/LCI technology has been realized since its first uses to improve data acquisition speed, size, and to enable *in vivo* capabilities. With these and other advances, the translation of the a/LCI technology from laboratory to clinical operation and ultimate deployment as a widely used cancer screening tool will continue.

## VALIDATION WITH ANIMAL MODELS

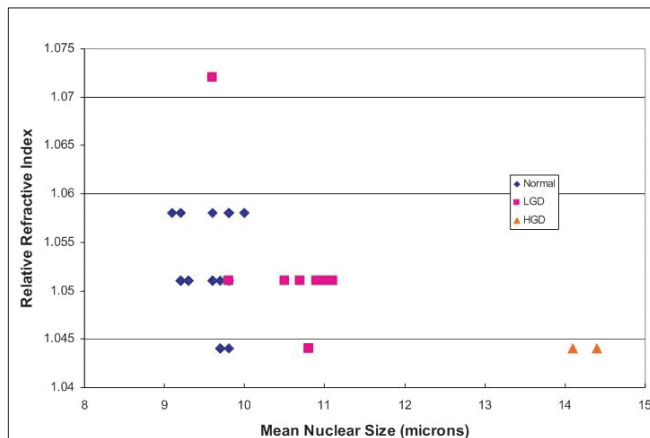
The first validation of a/LCI for detecting dysplasia in tissues came through two experiments with the rat esophageal carcinogenesis (REC) model. The initial study was retrospective and compared a/LCI nuclear morphology measurements with the histopathologic evaluation of tissue health. The second study used a decision line established in the first study to prospectively grade tissue samples.

The REC model employed male F344 rats, 4–5 weeks of age, obtained from Harlan Sprague Dawley (Indianapolis, IN, USA) for these experiments. Carcinogen-treated animals were given subcutaneous injections of *N*-nitrosomethylbenzylamine (NMBA; 0.25 mg/kg body weight), obtained from Ash Stevens, Inc. (Detroit, MI, USA), in the intrascapular region three times a week for 5 weeks with concentrations adjusted weekly based upon average body weight. The solvent for NMBA was 20% dimethyl sulfoxide (DMSO):H<sub>2</sub>O and the injection volume was 0.2 ml. Control groups received a similar injection regimen of 20% DMSO:H<sub>2</sub>O. At 8, 12, and 20 weeks after the initial injection of NMBA, NMBA-treated and control rats were harvested for a/LCI analysis. The rats were euthanized by CO<sub>2</sub> asphyxiation and subjected to gross necropsy. The entire esophagus was excised and opened longitudinally for immediate optical spectroscopic analysis. Following a/LCI analysis, the esophagus was fixed in 10% neutral buffered formalin. All of the experimental protocols were in accordance with NIH guidelines and approved by the Institutional Animal Care and Use Committees of Duke University.

Each of the a/LCI scans was processed and analyzed to determine the nuclear morphology of the associated sample. In early a/LCI tissue studies, the chief morphological descriptor used for classifying tissues was the mean size of the cell nuclei.<sup>[4,6,24]</sup> A later study retrospectively assessed the relative refractive index of the cell nuclei relative to the cytoplasm as to determine its diagnostic capacity as a biomarker.<sup>[25]</sup>

The first a/LCI study of rat esophagus showed an increase in mean nuclear size with neoplastic progression [Figure 3].<sup>[4]</sup> The average nuclear size in normal tissues was found to be  $9.55 \pm 0.23 \mu\text{m}$ , which increased to  $10.5 \pm 0.56 \mu\text{m}$  for low-grade dysplasia (LGD), and to  $14.4 \pm 0.21 \mu\text{m}$  for high-grade dysplasia (HGD). A statistically significant difference was found between the normal and LGD mean sizes ( $P < 0.001$ ), and between normal and abnormal (LGD+HGD) mean sizes ( $P < 0.005$ ). A decision threshold was established using logistic regression, which yielded 80% sensitivity and 100% specificity in distinguishing normal and dysplastic tissues. A later analysis of these data reported that the relative refractive index of the nuclei in normal tissues was found to be  $1.052 \pm 0.0051$  compared to  $1.049 \pm 0.0031$  for dysplastic tissues, but this change fell short of statistical significance ( $P = 0.07$ ).<sup>[25]</sup>

The second a/LCI study of rat esophagus prospectively used the decision line from the first study to classify tissues.<sup>[6]</sup> This study consisted of two cohorts of animals, the first examined with the first-generation time-domain a/LCI system and the second with the second-generation time-domain system. For the first cohort of animals, the mean nuclear diameter was found to be  $9.09 \pm 1.06 \mu\text{m}$  for the normal tissues and  $11.86 \pm 1.16 \mu\text{m}$  for the dysplastic tissues, with a highly statistically significant difference ( $P < 0.0001$ ). The relative refractive index of the nuclei in these tissues was found to be  $1.047 \pm 0.0051$  for the normal tissues and  $1.041 \pm 0.0038$  for the dysplastic tissues. This also had a highly statistically significant difference ( $P < 0.001$ ). In the second cohort of animals in this study, the mean nuclear diameter was found to be  $8.80 \pm 0.51 \mu\text{m}$  for normal tissues and  $12.07 \pm 1.73 \mu\text{m}$  for dysplastic tissues, again with a highly statistically significant difference ( $P < 0.0001$ ). The relative refractive index of the nuclei in these tissues was found to be  $1.057 \pm 0.0068$  for the normal tissues and  $1.051 \pm 0.0094$  for the dysplastic



### Ex vivo study

The endoscopic Fourier-domain a/LCI system was used to conduct a study of esophageal tissue samples from three BE patients who had undergone esophagogastrectomies.<sup>[11]</sup> This study provided the opportunity to perform an initial investigation into the performance of a/LCI when detecting dysplasia in human esophagus.

Within 2 hours of resection, each tissue sample was transported to the laboratory for analysis using the endoscopic a/LCI system. Each of the samples was scanned at multiple locations. Following scanning using the a/LCI system, tissue biopsies from these locations were evaluated by a pathologist. The collected scattering spectra were analyzed to determine the mean nuclear diameter and density of the corresponding tissue functions of epithelial depth. Trends in these metrics were correlated with the disease state of the tissue to assess the ability to detect dysplastic tissues.

Of the 18 tissue sites scanned, 5 were healthy gastric tissue while 13 were characterized by dysplastic BE tissue. For analysis, measurements taken across the superficial 150  $\mu\text{m}$  were averaged for each of the biopsy populations. For gastric tissue, the mean nuclear diameter was found to be 10.1  $\mu\text{m}$  while the relative refractive index of nuclei was found to be 1.05. For dysplastic tissue, these values changed to 12.9  $\mu\text{m}$  and 1.04, respectively. Both metrics were found to be statistically significant discriminators. When these two values were plotted together as seen in Figure 4, a clear delineation between the two populations was apparent.

While this study provided an encouraging initial result, it did have multiple limitations. The small number of patients and biopsies sampled were not sufficient to provide a definitive insight into the diagnostic power of the technique. In addition, no non-dysplastic BE tissue was available for analysis, a consequence of the severe disease state of the resected tissue samples that were analyzed. Furthermore, this non-portable and laboratory-based system was not appropriate for use in a clinical setting.

### Clinical ex vivo study

Following its technological development, the portable a/LCI system was used to conduct a clinical *ex vivo* study of BE patients.<sup>[16]</sup> In a manner similar to the previous study, this study examined resected esophageal tissue. In contrast, however, this study was conducted at the pathology laboratory using a handheld optical probe, which allowed for precise selection of tissue locations of interest.

In this study, tissue samples from a single segment of resected esophageal tissue were scanned at multiple tissue

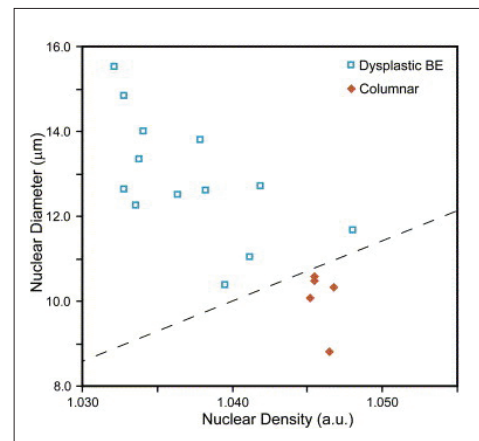


**Figure 4: Scatter plot of tissue samples scanned in primary ex vivo clinical study. Data points are colored according to pathologic diagnosis. Dashed black line indicates decision line (Taken from<sup>[11]</sup>)**

locations. Five and four data points were taken from healthy squamous and gastric tissue, respectively. In addition, six data points were taken from BE tissue with low-grade dysplasia. These data were analyzed in a similar manner to the previous study.

When data from the superficial 150  $\mu\text{m}$  of the epithelium were analyzed and stratified using a similar decision line used in the previous study, it once again provided good sensitivity (100%; 6/6). Unlike the previous study, however, the specificity of this measure was low (56%; 5/9). When the deeper segment of tissue, which contained the basal layer, was analyzed in the same manner, there was again excellent sensitivity (100%; 6/6) but also improved specificity (78%; 7/9). This result indicated that the deep basal layer might provide the greatest insight into the disease state of the tissue as measured by a/LCI.

This study was a significant step toward the development of a clinical diagnostic for the detection of esophageal dysplasia, but it too suffered from limitations. Again, the low number of tissue points sampled and the fact that all of these samples were taken from a single patient restricted the conclusions that could be drawn from this study. Also, the handheld probe and portable system allowed measurements to be taken in a clinical environment, but could not be used to take measurements of *in situ* epithelial tissue.

### In vivo clinical trial

By allowing measurements to be taken through the accessory channel of a standard endoscope, the clinical a/LCI system enabled the first-in-man pilot study to be conducted.<sup>[12]</sup> In this study, 46 consecutive patients undergoing routine upper endoscopy for BE were enrolled at two endoscopy centers. During these procedures, the a/LCI probe was inserted

through the endoscope's accessory channel and three to six tissue sites were scanned with the system. Following each of these optical biopsies, the probe was retracted and a co-registered standard biopsy was taken. Following pathological classification of these biopsies, the disease state of each tissue site was correlated with the a/LCI measurements in order to assess the diagnostic ability of a/LCI.

A total of 172 co-registered optical and physical biopsies were taken in this study. For analysis, these biopsies were dichotomized as "dysplastic" ( $n=13$ ) and "non-dysplastic" ( $n=159$ ) according to their pathologic state. When analyzed, increased nuclear diameter from the deep epithelial layer from 200 to 300  $\mu\text{m}$  in depth showed a strong statistical ( $P<0.001$ ) correlation with the presence of dysplasia, which was consistent with the results from the previous human a/LCI studies. To evaluate the diagnostic ability of this metric, a receiver operating characteristic (ROC) was developed. This showed good overall performance in discrimination, with an area under the curve (AUC) of 0.91, and identified an optimal decision line at 11.84  $\mu\text{m}$  for the classification of dysplasia. Shown in Figure 5, this decision line yielded a sensitivity of 100% (13/13), a specificity of 84% (134/159), an overall accuracy of 86% (147/172), and positive and negative predictive values of 34% (13/38) and 100% (134/134), respectively.

This pilot *in vivo* study represented a significant step in the development of a clinical diagnostic for dysplasia in the esophagus, and will serve as a proof-of-concept for future trials.

### Summary

The use of a/LCI nuclear morphology measurements has been developed as a tool for diagnosing dysplastic tissues without the need for acquiring a biopsy or the subsequent sample processing and evaluation. As described above, the approach was initially developed by assessing neoplastic changes in animal tissues, notably the REC model. The a/LCI method offers several benefits over traditional methods for evaluating neoplastic change in animal models. First, a/LCI provides information on tissue health without tissue fixation and processing such that further additional assays such as immunohistochemistry are not prevented. Another significant benefit is that a/LCI detects neoplastic changes earlier in animal models than other bioassay methods, such as tumor metrology measurements.<sup>[6]</sup> Finally, the richness of a/LCI nuclear morphology data can be exploited to gain information on cellular processes such as apoptosis,<sup>[4,6,24]</sup> suggesting that this approach can be used for studies which seek to evaluate the efficacy of chemopreventive and chemotherapeutic agents.

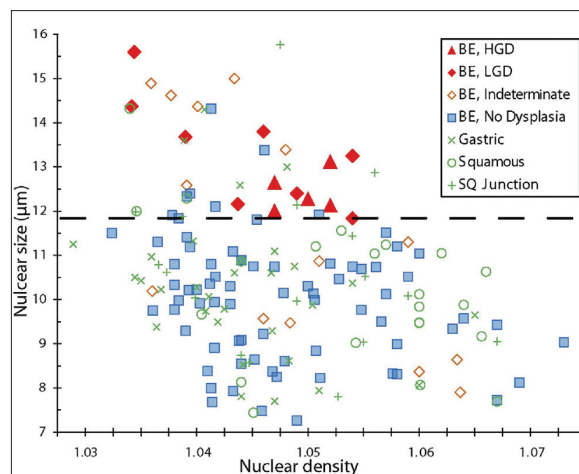


**Figure 5: Scatter plot of optical biopsies from pilot *in vivo* clinical study. Data points are colored according to pathologic diagnosis. Dashed black line indicates optimal decision line (Taken from <sup>[12]</sup>)**

To put a/LCI and its clinical potential in perspective, we consider here the development of other optical techniques for clinical utility in BE, using OCT and confocal endomicroscopy as examples, both of which are direct imaging modalities, producing images of the scanned tissues rather than the derived parameters of nuclear morphology measured with a/LCI. OCT relies on low coherence interferometry to obtain depth resolution, similar to a/LCI, and is capable of imaging greater than 1 mm in depth.<sup>[10]</sup> In general, its transverse and axial resolutions are in the range of 5–20  $\mu\text{m}$ , which permit characterization of structures at the tissue level but are insufficient to resolve subcellular details. Further, in direct imaging modalities, an experienced clinician is necessary to interpret the images based on tissue morphology to identify any indications of dysplasia. Several OCT-based BE studies have reported sensitivity and specificity in the 70–80% range.<sup>[32–35]</sup> For instance, a study in 2008 involving 78 patients and 181 biopsy sites produced 83% sensitivity and 68% specificity in identifying HGD, intramucosal adenocarcinoma, and invasive carcinoma in BE patients.<sup>[34]</sup>

As with OCT, confocal microendoscopy also provides direct images of tissue, which requires interpretation by an expert. Confocal imaging techniques can achieve micron-level resolution to resolve cellular morphology, which is believed to result in higher sensitivity and specificity in clinical studies.<sup>[36,37]</sup> A 63-patient study in 2006 was able to differentiate LGD, HGD and cancer with 92.9% sensitivity and 98.4% specificity.<sup>[37]</sup> However, unlike label-free methods, confocal microendoscopy requires the administration of fluorescence contrast agents, which limits the imaging flexibility during a procedure. Further, it can only visualize relatively shallow cellular structures up to

100–150  $\mu\text{m}$  below the tissue surface. This is in contrast to a/LCI studies which have shown that the basal layer of the epithelium, 250–300  $\mu\text{m}$  below the tissue surface, is most useful for detecting dysplasia when confounding factors such as inflammation are present.

In summary, we have reviewed the development of a/LCI for assessing neoplastic change based on *in situ* nuclear morphology measurements. The a/LCI method has been applied to evaluating neoplastic progression in studies of animal tissues, such as the REC model. These animal models provided a powerful means for validating the approach and justifying further development of the methods for *in vivo* clinical use. Successful translation of a/LCI to clinical applications has shown that the approach can be applied to detection of dysplasia in BE patients, addressing a significant unmet need. The results reviewed here suggest that a/LCI can serve as a powerful new method for evaluating the health of at-risk epithelial tissues in the clinic.

## ACKNOWLEDGMENTS

This work was supported by grants from the National Cancer Institute (NCI R21-CA109907, R33-109907, R01-CA138594), the National Science Foundation (BES 03-48204) and a grant from the Coulter Translational Partnership.

## REFERENCES

- Kalikin LM, Schneider A, Thakur MA, Fridman Y, Griffin LB, Dunn RL, et al. *In vivo* visualization of metastatic prostate cancer and quantitation of disease progression in immunocompromised mice. *Cancer Biol Ther* 2003;2:656-60.
- Choy G, O'Connor S, Diehn FE, Costouros N, Alexander HR, Choyke P, et al. Comparison of noninvasive fluorescent and bioluminescent small animal optical imaging. *Biotechniques* 2003;35:1022-30.
- Chen Y, Zheng G, Zhang ZH, Blessington D, Zhang M, Li H, et al. Metabolism-enhanced tumor localization by fluorescence imaging: *In vivo* animal studies. *Opt Lett* 2003;28:2070-2.
- Wax A, Yang C, Muller MG, Nines R, Boone CW, Steele VE, et al. *In situ* detection of neoplastic transformation and chemopreventive effects in rat esophagus epithelium using angle-resolved low-coherence interferometry. *Cancer Res* 2003;63:3556-9.
- Roy HK, Liu Y, Wali RK, Kim YL, Kromine AK, Goldberg MJ, et al. Four-dimensional elastic light-scattering fingerprints as preneoplastic markers in the rat model of colon carcinogenesis. *Gastroenterology* 2004;126:1071-81.
- Wax A, Pyhtila JW, Graf RN, Nines R, Boone CV, Dasari RR, et al. Prospective grading of neoplastic change in rat esophagus epithelium using angle-resolved low-coherence interferometry. *J Biomed Opt* 2005;10:051604.
- Robles F, Zhu Y, Lee J, Sharma S, Wax A. Fourier domain low coherence interferometry for detection of early colorectal cancer development in the azoxymethane rat carcinogenesis model. *Biomed Opt Express* 2010;1:736-45.
- Roy HK, Kim YL, Liu Y, Wali RK, Goldberg MJ, Turzhitsky V, et al. Risk stratification of colon carcinogenesis through enhanced backscattering spectroscopy analysis of the uninvolved colonic mucosa. *Clin Cancer Res* 2006;12:961-8.
- Izatt JA, Kulkarni MD, Wang HW, Kobayashi K, Sivak MV. Optical coherence tomography and microscopy in gastrointestinal tissues. *IEEE J Sel Top Quantum Electron* 1996;2:1017-28.
- Huang D, Swanson EA, Lin CP, Schuman JS, Stinson WG, Chang W, et al. Optical coherence tomography. *Science* 1991;254:1178-81.
- Pyhtila JW, Chalut KJ, Boyer JD, Keener J, D'Amico T, Gottfried M, et al. *In situ* detection of nuclear atypia in Barrett's esophagus by using angle-resolved low-coherence interferometry. *Gastrointest Endosc* 2007;65:487-91.
- Terry NG, Zhu Y, Rinehart MT, Brown WJ, Gebhart SC, Bright S, et al. Detection of Dysplasia in Barrett's Esophagus With *In Vivo* Depth-Resolved Nuclear Morphology Measurements. *Gastroenterology* 2011;140:42-50.
- Wax A, Yang C, Backman V, Kalashnikov M, Dasari RR, Feld MS. Determination of particle size by using the angular distribution of backscattered light as measured with low-coherence interferometry. *J Opt Soc Am A* 2002;19:737-44.
- Wax A, Yang CH, Backman V, Badizadegan K, Boone CW, Dasari RR, et al. Cellular organization and substructure measured using angle-resolved low-coherence interferometry. *Biophys J* 2002;82:2256-64.
- Pyhtila JW, Graf RN, Wax A. Determining nuclear morphology using an improved angle-resolved low coherence interferometry system. *Opt Express* 2003;11:3473-84.
- Brown WJ, Pyhtila JW, Terry NG, Chalut KJ, D'Amico TA, Sporn TA, et al. Review and recent development of angle-resolved low-coherence interferometry for detection of precancerous cells in human esophageal epithelium. *IEEE J Sel Top Quantum Electron* 2008;14:88-97.
- van de Hulst HC. *Light scattering by small particles*. United States: Dover Publications; 1981.
- Perelman LT, Backman V, Wallace M, Zonios G, Manoharan R, Nusrat A, et al. Observation of periodic fine structure in reflectance from biological tissue: A new technique for measuring nuclear size distribution. *Phys Rev Lett* 1998;80:627-30.
- Chalut KJ, Chen S, Finan JD, Giacomelli MG, Guilak F, Leong KW, et al. Label-free, high-throughput measurements of dynamic changes in cell nuclei using angle-resolved low coherence interferometry. *Biophys J* 2008;94:4948-56.
- Wilson JD, Foster TH. Mie theory interpretations of light scattering from intact cells. *Opt Lett* 2005;30:2442-4.
- Smith ZJ, Berger AJ. Validation of an integrated Raman- and angular-scattering microscopy system on heterogeneous bead mixtures and single human immune cells. *Appl Opt* 2009;48:D109-20.
- Steinke JM, Shepherd AP. Comparison of mie theory and the light-scattering of red blood-cells. *Appl Opt* 1988;27:4027-33.
- Yu CC, Lau C, Tunnell JW, Hunter M, Kalashnikov M, Fang-Yen C. Assessing epithelial cell nuclear morphology by using azimuthal light scattering spectroscopy. *Opt Lett* 2006;31:3119-21.
- Chalut KJ, Ostrander JH, Giacomelli MG, Wax A. Light Scattering Measurements of Subcellular Structure Provide Noninvasive Early Detection of Chemotherapy-Induced Apoptosis. *Cancer Res* 2009;69:1199-204.
- Wax A, Pyhtila JW. *In situ* nuclear morphology measurements using light scattering as biomarkers of neoplastic change in animal models of carcinogenesis. *Dis Markers* 2008;25:291-301.
- Chalut KJ, Kresty LA, Pyhtila JW, Nines R, Baird M, Steele VE, et al. *In situ* assessment of intraepithelial neoplasia in hamster trachea epithelium using angle-resolved low-coherence interferometry. *Cancer Epidemiol Biomark Prev* 2007;16:223-7.
- Choma MA, Sarunic MV, Yang CH, Izatt JA. Sensitivity advantage of swept source and Fourier domain optical coherence tomography. *Opt Express* 2003;11:2183-9.
- Pyhtila JW, Wax A. Rapid, depth-resolved light scattering measurements using Fourier domain, angle-resolved low coherence interferometry. *Opt Express* 2004;12:6178-83.
- Pyhtila JW, Boyer JD, Chalut KJ, Wax A. Fourier-domain angle-resolved low coherence interferometry through an endoscopic fiber bundle for light-scattering spectroscopy. *Opt Lett* 2006;31:772-4.
- Zhu YZ, Terry NG, Woosley JT, Shaheen NJ, Wax A. Design and validation of an angle-resolved low-coherence interferometry fiber probe for *in vivo* clinical measurements of depth-resolved nuclear morphology. *J Biomed Opt* 2011;16:011003.
- Giacomelli MG, Chalut KJ, Ostrander JH, Wax A. Review of the Application of T-Matrix Calculations for Determining the Structure of Cell Nuclei With Angle-Resolved Light Scattering Measurements. *IEEE J Sel Top Quantum Electron* 2010;16:900-8.
- Isenberg G, Sivak MV Jr, Chak A, Wong RC, Willis JE, Wolf B, et al. Accuracy of endoscopic optical coherence tomography in the detection of dysplasia in Barrett's esophagus: A prospective, double-blinded study. *Gastrointest*

- Endosc 2005;62:825-31.
33. Evans JA, Poneroy JM, Bouma BE, Bressner J, Halpern EF, Shishkov M, et al. Optical coherence tomography to identify intramucosal carcinoma and high-grade dysplasia in Barrett's esophagus. *Clin Gastroenterol Hepatol* 2006;4:38-43.
  34. Zagaynova E, Gladkova N, Shakhova N, Gelikonov G, Gelikonov V. Endoscopic OCT with forward-looking probe: Clinical studies in urology and gastroenterology. *J Biophotonics* 2008;1:114-28.
  35. Qi X, Pan Y, Sivak MV, Willis JE, Isenberg G, Rollins AM. Image analysis for classification of dysplasia in Barrett's esophagus using endoscopic optical coherence tomography. *Biomed Opt Express* 2010;1:825-47.
  36. Pohl H, Rosch T, Vieth M, Koch M, Becker V, Anders M, et al. Miniprobe confocal laser microscopy for the detection of invisible neoplasia in patients with Barrett's oesophagus. *Gut* 2008;57:1648-53.
  37. Kiesslich R, Gossner L, Goetz M, Dahmann A, Vieth M, Stolte M, et al. *In vivo* histology of Barrett's esophagus and associated neoplasia by confocal laser endomicroscopy. *Clin Gastroenterol Hepatol* 2006;4:979-87.

---

## Author's Profile

**Dr. Yizheng Zhu**, Research Scientist, Department of Biomedical Engineering, Duke University, USA.

**Dr. Neil G. Terry**, Department of Biomedical Engineering, Duke University, USA.

**Dr. Adam Wax**, Associate Professor, Department of Biomedical Engineering, Duke University, USA.



Journal of Carcinogenesis is published for Carcinogenesis Press by Medknow Publications and Media Pvt. Ltd.

Manuscripts submitted to the journal are peer reviewed and published immediately upon acceptance, cited in PubMed and archived on PubMed Central. Your research papers will be available free of charge to the entire biomedical community. Submit your next manuscript to Journal of Carcinogenesis.

[www.journalonweb.com/jcar/](http://www.journalonweb.com/jcar/)